in various normal tissues and involved in the pharmacokinetics of a wide range of drugs, mediating the efflux of drugs from the intracellular to the extracellular space [73]. Many isoforms of ABC drug transporters have been isolated and characterized. Currently, the ABC superfamily is designated based on the sequence and organization of their ATP-binding domains, representing the largest family of TM proteins (e.g., transporters, ion channels, and receptors). This family is subdivided based on similarities in domain structure, nucleotide-binding folds, and TM domains [74]. Of the 48 members identified to date, several members are well characterized as drug transporters. P-gp/MDR1 is now designated as ABCB1. MDR3 (ABCB4) and BSEP (bile salt export pump or sister P-gp, ABCB11) are included in the ABCB subfamily. The MRP subfamily includes MRP1 (ABCC1), MRP2 (ABCC2), MRP3 (ABCC3), MRP4 (ABCC4), and other MRP isoforms [75]. Other members of the ABCC subfamily include CFTR (cystic fibrosis transmembrane conductance regulator, a Cl^- channel) and SUR1 and SUR2 (sulfonylurea receptors). BCRP (ABCG2) belongs to a different subfamily known as the White subfamily [76]. The clinical relevance of P-gp has been demonstrated in terms of drug interaction, gene polymorphisms, and expression levels.

The general structure of ABC transporters comprises 12 TM regions, split into two halves, each with a nucleotide-binding domain (NBD) [77]. However, there are a number of exceptions to this arrangement. For example, MRP1–3 have an additional five TM regions at the N terminus. BCRP has only six TM regions and one NBD and is known as a half transporter. In general, ABC transporters are expressed in blood–tissue barriers such as the blood–brain barrier and at the luminal surface of epithelial cells such as intestinal epithelial cells to protect the cells from toxic substances.

23.3.5.2. Function and Pharmacokinetic Roles

23.3.5.2.1. MDR1 (P-GP and ABCB1): P-gp has an extremely broad substrate specificity, with a tendency towards lipophilic, cationic compounds. The list of its substrates/inhibitors is continually growing and includes anticancer agents, antibiotics, antivirals, calcium channel blockers, and immunosuppressive agents. Its physiological function was clearly demonstrated by creating an *Mdr1a/1b*$^{-/-}$ mouse [78]. Studies in vivo using this mouse model revealed that MDR1 functions as a gatekeeper of the blood–brain barrier, blood–placental barrier, blood–testis barrier, and gut [79, 80]. P-gp is expressed at brush-border membranes of enterocytes, where it functions as the efflux pump for xenobiotics in the intestinal lumen before they can access the portal circulation.

The antituberculosis drug rifampicin (rifampin) is known to affect a number of drug-metabolizing enzymes such as cytochrome P450 (CYP) 3A4 in the liver and in the small intestine, causing a loss of efficacy of drugs metabolized by CYP3A4. In addition, rifampicin induces the intestinal expression of P-gp, decreasing the oral bioavailability of P-gp substrates such as digoxin [81] and talinorol [82]. Not only drugs but also herbal products, that is, St. John's wort, administered for a long term have been shown to induce the intestinal expression of CYP3A and P-gp, consistent with the loss of efficacy of various drug therapies in earlier case reports and specific clinical studies [83].

The expression level of intestinal MDR1 mRNA has been utilized to the personalized immunosuppressant therapy with tacrolimus in cases of living-donor liver transplantation (LDLT) [84]. Tacrolimus shows wide

intra- and interindividual pharmacokinetic variability, especially in bioavailability after oral administration. P-gp and CYP3A4 are suggested to cooperate in the intestinal absorption of tacrolimus. Our laboratories reported an inverse correlation between the tacrolimus concentration/dose (C/D) ratio and the intestinal mRNA level of MDR1 ($r = -0.776$), but not of CYP3A4 ($r = -0.096$), in 46 cases [85] which was confirmed in studies with a larger population ($r = -0.645$, $n = 104$) [86]. Furthermore, a higher level of intestinal MDR1 expression was strongly associated with the probability of acute cellular rejection (ACR), but there was no significant association between the intestinal CYP3A4 mRNA level and ACR. These results indicate that the expression level of intestinal MDR1 mRNA found with LDLT is not only a pharmacokinetic factor, but also a significant biomarker for ACR [87].

23.3.5.2.2. MRP2 (ABCC2): MRP2 was first functionally characterized as a canalicular multispecific organic anion transporter in canalicular membranes of hepatocytes [88]. This transporter can accept a diverse range of substrates, including glutathione, glucuronide, and sulfate conjugates of many endo- and xenobiotics and expressed at the apical domain of hepatocytes, enterocytes of the proximal small intestine and proximal renal tubular cells, as well as in the brain and placenta. Mutation of MRP2 causes the Dubin-Johnson syndrome [89].

23.3.5.2.3. MRP3 (ABCC3): In contrast to other ABC drug transporters, MRP3 is mainly expressed at basolateral membranes of epithelial cells in the liver and intestine [90]. Substrates for MRP3 include glucuronosyl and sulfated conjugates, whereas glutathione conjugates are relatively poor substrates for MRP3 compared with MRP1 and MRP2 [91]. As MRP3 also transports some bile salts [92], this transporter has been believed to play important roles in the enterohepatic circulation of bile salts by transporting them from enterocytes into the circulating blood to prevent the accumulation of intracellular bile acids. Mice lacking *Mrp3* were recently developed which are viable and fertile, exhibiting no apparent phenotype [93].

23.3.5.2.4. BCRP (ABCG2): Unlike P-gp and MRPs, BCRP has only one ABC and six putative TM domains, and therefore, is referred to as a half-ABC transporter, most likely functioning as a homodimer [76]. Among human tissues, the placenta showed the highest level of BCRP mRNA, followed by the liver and small intestine [94]. Unlike humans, mice exhibited high levels of mRNA in the kidney and only moderate levels in the placenta [95]. BCRP is capable of transporting a diverse array of substrates, which overlap those of P-gp and MRP1 to a certain extent [76]. Using mice lacking Bcrp, it was demonstrated that this transporter protects against the gastrointestinal absorption of a potent phototoxic agent, pheophorbide [96]. BCRP also mediates the intestinal efflux of an antibiotic, nitrofurantoin [97].

23.4. Conclusions and Perspectives

In this chapter, basic characteristics of major drug transporters and their preclinical/clinical implications are discussed. During the past 10 years, molecular information on each transporter has been organized. Novel technologies and various useful public databases such as SNP have improved our understanding

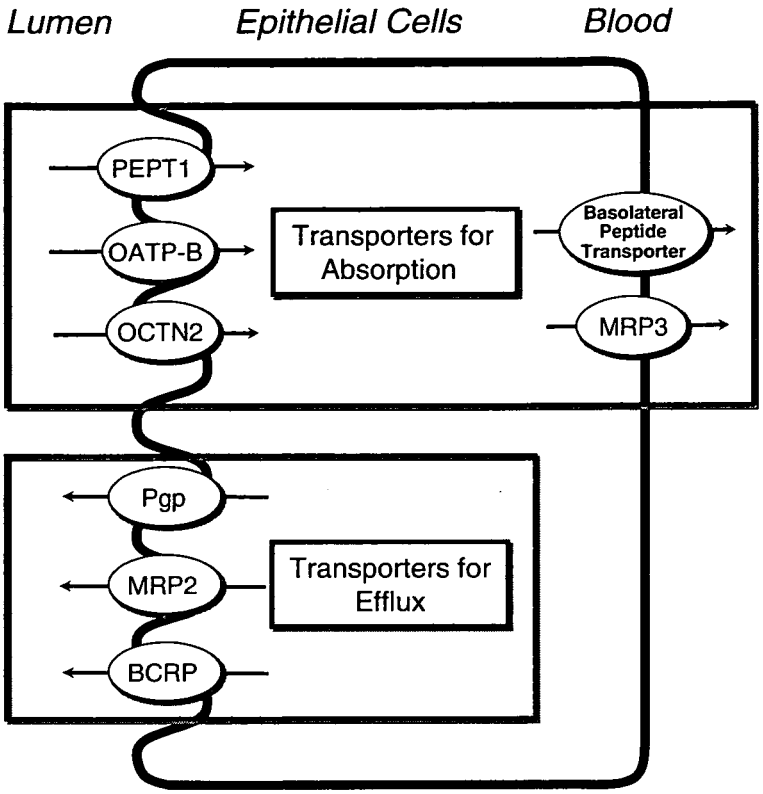

Figure 23.3 Drug transporters in the intestinal epithelial cells. PEPT1 is the most characterized transporter for intestinal drug absorption. The basolateral peptide transporter, which is not identified at the molecular level, also plays important roles. OATP-B, OCTN2 and MRP3 may be responsible for the intestinal absorption of some drugs. On the contrary, ABC transporters such as P-gp located at brush-border membranes mediated the efflux of drugs from intestinal epithelial cells, contributing to the low bioavailability of drugs such as the immunosuppressive agent, tacrolimus.

of the physiological, pharmacokinetic, and pharmacotherapeutic roles of these drug transporters. Drug transporter research can be actually applied to clinical science and drug development; that is, applications of drug delivery, the clarification of drug/drug interactions, application of personalized pharmacotherapy, and clarification of the relationship of each transporter to particular disease(s).

Various drug transporters are responsible for determining the oral bioavailability of drugs (Figure 23.3), although the extent of their contribution to the overall intestinal absorption process in vivo is not clear in some cases. Among them, peptide transporters, P-gp, MRP2, and BCRP unequivocally function as important factors regulating the oral bioavailability of drugs. Molecular determination of absorption by peptide transporters or secretion/excretion by ABC drug transporters will contribute to help the oral bioavailability of drugs under study.

Acknowledgments: This work was supported by the 21st Century COE Program "Knowledge Information Infrastructure for Genome Science", a Grant-in-Aid from the Japan Health Sciences Foundation and a Grant-in-Aid for Research on Advanced Medical Technology from the Ministry of Health, Labor and Welfare of Japan.

References

1. Y. J. Fei, Y. Kanai, S. Nussberger, V. Ganapathy, F. H. Leibach, M. F. Romero, S. K. Singh, W. F. Boron, and M. A. Hediger. Expression cloning of a mammalian proton-coupled oligopeptide transporter. *Nature* **368**: 563–566 (1994).
2. S. Ramamoorthy, W. Liu, Y. Y. Ma, T. L. Yang-Feng, V. Ganapathy, and F. H. Leibach. Proton/peptide cotransporter (PEPT 2) from human kidney: functional characterization and chromosomal localization. *Biochim Biophys Acta* **1240**: 1–4 (1995).

3. H. Saito, M. Okuda, T. Terada, S. Sasaki, and K. Inui. Cloning and characterization of a rat H^+/peptide cotransporter mediating absorption of beta-lactam antibiotics in the intestine and kidney. *J Pharmacol Exp Ther* **275**: 1631–1637 (1995).
4. H. Saito, T. Terada, M. Okuda, S. Sasaki, and K. Inui. Molecular cloning and tissue distribution of rat peptide transporter PEPT2. *Biochim Biophys Acta* **1280**: 173–177 (1996).
5. H. Ogihara, H. Saito, B. C. Shin, T. Terado, S. Takenoshita, Y. Nagamachi, K. Inui, and K. Takata. Immuno-localization of H^+/peptide cotransporter in rat digestive tract. *Biochem Biophys Res Commun* **220**: 848–852 (1996).
6. H. Daniel. Molecular and integrative physiology of intestinal peptide transport. *Annu Rev Physiol* **66**: 361–384 (2004).
7. T. Terada, and K. Inui. Peptide transporters: structure, function, regulation and application for drug delivery. *Curr Drug Metab* **5**: 85–94 (2004).
8. F. Doring, J. Walter, J. Will, M. Focking, M. Boll, S. Amasheh, W. Clauss, and H. Daniel. Delta-aminolevulinic acid transport by intestinal and renal peptide transporters and its physiological and clinical implications. *J Clin Invest* **101**: 2761–2767 (1998).
9. F. Doring, J. Will, S. Amasheh, W. Clauss, H. Ahlbrecht, and H. Daniel. Minimal molecular determinants of substrates for recognition by the intestinal peptide transporter. *J Biol Chem* **273**: 23211–23218 (1998).
10. H. Han, R. L. de Vrueh, J. K. Rhie, K. M. Covitz, P. L. Smith, C. P. Lee, D. M. Oh, W. Sadee, and G. L. Amidon. 5′-Amino acid esters of antiviral nucleosides, acyclovir, and AZT are absorbed by the intestinal PEPT1 peptide transporter. *Pharm Res* **15**: 1154–1159 (1998).
11. K. Sawada, T. Terada, H. Saito, Y. Hashimoto, and K. Inui. Recognition of L-amino acid ester compounds by rat peptide transporters PEPT1 and PEPT2. *J Pharmacol Exp Ther* **291**: 705–709 (1999).
12. M. Sugawara, W. Huang, Y. J. Fei, F. H. Leibach, V. Ganapathy, and M. E. Ganapathy. Transport of valganciclovir, a ganciclovir prodrug, via peptide transporters PEPT1 and PEPT2. *J Pharm Sci* **89**: 781–789 (2000).
13. M. Irie, T. Terada, T. Katsura, S. Matsuoka, and K. Inui. Computational modelling of H^+-coupled peptide transport via human PEPT1. *J Physiol* **565**: 429–439 (2005).
14. M. Sala-Rabanal, D. D. Loo, B. A. Hirayama, E. Turk, and E. M. Wright. Molecular interactions between dipeptides, drugs and the human intestinal H^+-oligopeptide cotransporter hPEPT1. *J Physiol* **574**: 149–166 (2006).
15. X. Song, P. L. Lorenzi, C. P. Landowski, B. S. Vig, J. M. Hilfinger, and G. L. Amidon. Amino acid ester prodrugs of the anticancer agent gemcitabine: synthesis, bioconversion, metabolic bioevasion, and hPEPT1-mediated transport. *Mol Pharm* **2**: 157–167 (2005).
16. C. P. Landowski, X. Song, P. L. Lorenzi, J. M. Hilfinger, and G. L. Amidon. Floxuridine amino acid ester prodrugs: enhancing Caco-2 permeability and resistance to glycosidic bond metabolism. *Pharm Res* **22**: 1510–1518 (2005).
17. F. Li, L. Hong, C. I. Mau, R. Chan, T. Hendricks, C. Dvorak, C. Yee, J. Harris, and T. Alfredson. Transport of levovirin prodrugs in the human intestinal Caco-2 cell line. *J Pharm Sci* **95**: 1318–1325 (2006).
18. M. Tsuda, T. Terada, M. Irie, T. Katsura, A. Niida, K. Tomita, N. Fujii, and K. Inui. Transport characteristics of a novel peptide transporter 1 substrate, antihypotensive drug midodrine, and its amino acid derivatives. *J Pharmacol Exp Ther* **318**: 455–460 (2006).
19. E. Jacquemin, B. Hagenbuch, B. Stieger, A. W. Wolkoff, and P. J. Meier. Expression cloning of a rat liver Na^+-independent organic anion transporter. *Proc Natl Acad Sci U S A* **91**: 133–137 (1994).
20. B. Hagenbuch, and P. J. Meier. The superfamily of organic anion transporting polypeptides. *Biochim Biophys Acta* **1609**: 1–18 (2003).

21. B. Hagenbuch, and P. J. Meier. Organic anion transporting polypeptides of the OATP/SLC21 family: phylogenetic classification as OATP/SLCO superfamily, new nomenclature and molecular/functional properties. *Pflugers Arch* **447**: 653–665 (2004).
22. I. Tamai, J. Nezu, H. Uchino, Y. Sai, A. Oku, M. Shimane, and A. Tsuji. Molecular identification and characterization of novel members of the human organic anion transporter (OATP) family. *Biochem Biophys Res Commun* **273**: 251–260 (2000).
23. M. Iwai, H. Suzuki, I. Ieiri, K. Otsubo, and Y. Sugiyama. Functional analysis of single nucleotide polymorphisms of hepatic organic anion transporter OATP1B1 (OATP-C). *Pharmacogenetics* **14**: 749–757 (2004).
24. L. Liu, Y. Cui, A. Y. Chung, Y. Shitara, Y. Sugiyama, D. Keppler, and K. S. Pang. Vectorial transport of enalapril by Oatp1a1/Mrp2 and OATP1B1 and OATP1B3/MRP2 in rat and human livers. *J Pharmacol Exp Ther* **318**: 395–402 (2006).
25. W. Yamashiro, K. Maeda, M. Hirouchi, Y. Adachi, Z. Hu, and Y. Sugiyama. Involvement of transporters in the hepatic uptake and biliary excretion of valsartan, a selective antagonist of the angiotensin II AT1-receptor, in humans. *Drug Metab Dispos* **34**: 1247–1254 (2006).
26. Y. Nishizato, I. Ieiri, H. Suzuki, M. Kimura, K. Kawabata, T. Hirota, H. Takane, S. Irie, H. Kusuhara, Y. Urasaki, A. Urae, S. Higuchi, K. Otsubo, and Y. Sugiyama. Polymorphisms of OATP-C (SLC21A6) and OAT3 (SLC22A8) genes: consequences for pravastatin pharmacokinetics. *Clin Pharmacol Ther* **73**: 554–565 (2003).
27. M. Niemi, E. Schaeffeler, T. Lang, M. F. Fromm, M. Neuvonen, C. Kyrklund, J. T. Backman, R. Kerb, M. Schwab, P. J. Neuvonen, M. Eichelbaum, and K. T. Kivisto. High plasma pravastatin concentrations are associated with single nucleotide polymorphisms and haplotypes of organic anion transporting polypeptide-C (OATP-C, SLCO1B1). *Pharmacogenetics* **14**: 429–440 (2004).
28. M. Niemi, P. J. Neuvonen, U. Hofmann, J. T. Backman, M. Schwab, D. Lutjohann, K. von Bergmann, M. Eichelbaum, and K. T. Kivisto. Acute effects of pravastatin on cholesterol synthesis are associated with SLCO1B1 (encoding OATP1B1) haplotype *17. *Pharmacogenet Genomics* **15**: 303–309 (2005).
29. K. Maeda, I. Ieiri, K. Yasuda, A. Fujino, H. Fujiwara, K. Otsubo, M. Hirano, T. Watanabe, Y. Kitamura, H. Kusuhara, and Y. Sugiyama. Effects of organic anion transporting polypeptide 1B1 haplotype on pharmacokinetics of pravastatin, valsartan, and temocapril. *Clin Pharmacol Ther* **79**: 427–439 (2006).
30. M. Niemi, J. T. Backman, L. I. Kajosaari, J. B. Leathart, M. Neuvonen, A. K. Daly, M. Eichelbaum, K. T. Kivisto, and P. J. Neuvonen. Polymorphic organic anion transporting polypeptide 1B1 is a major determinant of repaglinide pharmacokinetics. *Clin Pharmacol Ther* **77**: 468–478 (2005).
31. D. A. Katz, R. Carr, D. R. Grimm, H. Xiong, R. Holley-Shanks, T. Mueller, B. Leake, Q. Wang, L. Han, P. G. Wang, T. Edeki, L. Sahelijo, T. Doan, A. Allen, B. B. Spear, and R. B. Kim. Organic anion transporting polypeptide 1B1 activity classified by SLCO1B1 genotype influences atrasentan pharmacokinetics. *Clin Pharmacol Ther* **79**: 186–196 (2006).
32. D. Kobayashi, T. Nozawa, K. Imai, J. Nezu, A. Tsuji, and I. Tamai. Involvement of human organic anion transporting polypeptide OATP-B (SLC21A9) in pH-dependent transport across intestinal apical membrane. *J Pharmacol Exp Ther* **306**: 703–708 (2003).
33. T. Nozawa, K. Imai, J. Nezu, A. Tsuji, and I. Tamai. Functional characterization of pH-sensitive organic anion transporting polypeptide OATP-B in human. *J Pharmacol Exp Ther* **308**: 438–445 (2004).

34. D. Gründemann, V. Gorboulev, S. Gambaryan, M. Veyhl, and H. Koepsell. Drug excretion mediated by a new prototype of polyspecific transporter. *Nature* **372**: 549–552 (1994).
35. M. Okuda, H. Saito, Y. Urakami, M. Takano, and K. Inui. cDNA cloning and functional expression of a novel rat kidney organic cation transporter, OCT2. *Biochem Biophys Res Commun* **224**: 500–507 (1996).
36. I. Tamai, H. Yabuuchi, J. Nezu, Y. Sai, A. Oku, M. Shimane, and A. Tsuji. Cloning and characterization of a novel human pH-dependent organic cation transporter, OCTN1. *FEBS Lett* **419**: 107–111 (1997).
37. T. Sekine, N. Watanabe, M. Hosoyamada, Y. Kanai, and H. Endou. Expression cloning and characterization of a novel multispecific organic anion transporter. *J Biol Chem* **272**: 18526–18529 (1997).
38. D. Gründemann, B. Schechinger, G. A. Rappold, and E. Schomig. Molecular identification of the corticosterone-sensitive extraneuronal catecholamine transporter. *Nat Neurosci* **1**: 349–351 (1998).
39. R. Kekuda, P. D. Prasad, X. Wu, H. Wang, Y. J. Fei, F. H. Leibach, and V. Ganapathy. Cloning and functional characterization of a potential-sensitive, polyspecific organic cation transporter (OCT3) most abundantly expressed in placenta. *J Biol Chem* **273**: 15971–15979 (1998).
40. I. Tamai, R. Ohashi, J. Nezu, H. Yabuuchi, A. Oku, M. Shimane, Y. Sai, and A. Tsuji. Molecular and functional identification of sodium ion-dependent, high affinity human carnitine transporter OCTN2. *J Biol Chem* **273**: 20378–20382 (1998).
41. X. Wu, P. D. Prasad, F. H. Leibach, and V. Ganapathy. cDNA sequence, transport function, and genomic organization of human OCTN2, a new member of the organic cation transporter family. *Biochem Biophys Res Commun* **246**: 589–595 (1998).
42. T. Sekine, S. H. Cha, M. Tsuda, N. Apiwattanakul, N. Nakajima, Y. Kanai, and H. Endou. Identification of multispecific organic anion transporter 2 expressed predominantly in the liver. *FEBS Lett* **429**: 179–182 (1998).
43. H. Kusuhara, T. Sekine, N. Utsunomiya-Tate, M. Tsuda, R. Kojima, S. H. Cha, Y. Sugiyama, Y. Kanai, and H. Endou. Molecular cloning and characterization of a new multispecific organic anion transporter from rat brain. *J Biol Chem* **274**: 13675–13680 (1999).
44. S. H. Cha, T. Sekine, H. Kusuhara, E. Yu, J. Y. Kim, D. K. Kim, Y. Sugiyama, Y. Kanai, and H. Endou. Molecular cloning and characterization of multispecific organic anion transporter 4 expressed in the placenta. *J Biol Chem* **275**: 4507–4512 (2000).
45. A. Enomoto, H. Kimura, A. Chairoungdua, Y. Shigeta, P. Jutabha, S. H. Cha, M. Hosoyamada, M. Takeda, T. Sekine, T. Igarashi, H. Matsuo, Y. Kikuchi, T. Oda, K. Ichida, T. Hosoya, K. Shimokata, T. Niwa, Y. Kanai, and H. Endou. Molecular identification of a renal urate anion exchanger that regulates blood urate levels. *Nature* **417**: 447–452 (2002).
46. H. Koepsell, and H. Endou. The SLC22 drug transporter family. *Pflugers Arch* **447**: 666–676 (2004).
47. K. Inui, S. Masuda, and H. Saito. Cellular and molecular aspects of drug transport in the kidney. *Kidney Int* **58**: 944–958 (2000).
48. S. H. Wright, and W. H. Dantzler. Molecular and cellular physiology of renal organic cation and anion transport. *Physiol Rev* **84**: 987–1049 (2004).
49. B. C. Burckhardt, and G. Burckhardt. Transport of organic anions across the basolateral membrane of proximal tubule cells. *Rev Physiol Biochem Pharmacol* **146**: 95–158 (2003).
50. M. A. Hediger, R. J. Johnson, H. Miyazaki, and H. Endou. Molecular physiology of urate transport. *Physiology (Bethesda)* **20**: 125–133 (2005).

51. R. R. Ramsay, R. D. Gandour, and F. R. van der Leij. Molecular enzymology of carnitine transfer and transport. *Biochim Biophys Acta* **1546**: 21–43 (2001).
52. Y. Urakami, N. Kimura, M. Okuda, and K. Inui. Creatinine transport by basolateral organic cation transporter hOCT2 in the human kidney. *Pharm Res* **21**: 976–981 (2004).
53. G. Ciarimboli, T. Ludwig, D. Lang, H. Pavenstadt, H. Koepsell, H. J. Piechota, J. Haier, U. Jaehde, J. Zisowsky, and E. Schlatter. Cisplatin nephrotoxicity is critically mediated via the human organic cation transporter 2. *Am J Pathol* **167**: 1477–1484 (2005).
54. A. Yonezawa, S. Masuda, K. Nishihara, I. Yano, T. Katsura, and K. Inui. Association between tubular toxicity of cisplatin and expression of organic cation transporter rOCT2 (Slc22a2) in the rat. *Biochem Pharmacol* **70**: 1823–1831 (2005).
55. H. Shimada, B. Moewes, and G. Burckhardt. Indirect coupling to Na^+ of p-aminohippuric acid uptake into rat renal basolateral membrane vesicles. *Am J Physiol* **253**: F795–F801 (1987).
56. T. Cihlar, D. C. Lin, J. B. Pritchard, M. D. Fuller, D. B. Mendel, and D. H. Sweet. The antiviral nucleotide analogs cidofovir and adefovir are novel substrates for human and rat renal organic anion transporter 1. *Mol Pharmacol* **56**: 570–580 (1999).
57. H. Motohashi, Y. Uwai, K. Hiramoto, M. Okuda, and K. Inui. Different transport properties between famotidine and cimetidine by human renal organic ion transporters (SLC22A). *Eur J Pharmacol* **503**: 25–30 (2004).
58. H. Ueo, H. Motohashi, T. Katsura, and K. Inui. Human organic anion transporter hOAT3 is a potent transporter of cephalosporin antibiotics, in comparison with hOAT1. *Biochem Pharmacol* **70**: 1104–1113 (2005).
59. Y. Sakurai, H. Motohashi, K. Ogasawara, T. Terada, S. Masuda, T. Katsura, N. Mori, M. Matsuura, T. Doi, A. Fukatsu, and K. Inui. Pharmacokinetic significance of renal OAT3 (SLC22A8) for anionic drug elimination in patients with mesangial proliferative glomerulonephritis. *Pharm Res* **22**: 2016–2022 (2005).
60. Y. Sakurai, H. Motohashi, H. Ueo, S. Masuda, H. Saito, M. Okuda, N. Mori, M. Matsuura, T. Doi, A. Fukatsu, O. Ogawa, and K. Inui. Expression levels of renal organic anion transporters (OATs) and their correlation with anionic drug excretion in patients with renal diseases. *Pharm Res* **21**: 61–67 (2004).
61. T. Terada, Y. Shimada, X. Pan, K. Kishimoto, T. Sakurai, R. Doi, H. Onodera, T. Katsura, M. Imamura, and K. Inui. Expression profiles of various transporters for oligopeptides, amino acids and organic ions along the human digestive tract. *Biochem Pharmacol* **70**: 1756–1763 (2005).
62. Y. Kato, M. Sugiura, T. Sugiura, T. Wakayama, Y. Kubo, D. Kobayashi, Y. Sai, I. Tamai, S. Iseki, and A. Tsuji. Organic cation/carnitine transporter octn2 (slc22a5) is responsible for carnitine transport across apical membranes of small intestinal epithelial cells in mouse. *Mol Pharmacol* **70**: 829–837 (2006).
63. J. Nezu, I. Tamai, A. Oku, R. Ohashi, H. Yabuuchi, N. Hashimoto, H. Nikaido, Y. Sai, A. Koizumi, Y. Shoji, G. Takada, T. Matsuishi, M. Yoshino, H. Kato, T. Ohura, G. Tsujimoto, J. Hayakawa, M. Shimane, and A. Tsuji. Primary systemic carnitine deficiency is caused by mutations in a gene encoding sodium ion-dependent carnitine transporter. *Nat Genet* **21**: 91–94 (1999).
64. S. Tokuhiro, R. Yamada, X. Chang, A. Suzuki, Y. Kochi, T. Sawada, M. Suzuki, M. Nagasaki, M. Ohtsuki, M. Ono, H. Furukawa, M. Nagashima, S. Yoshino, A. Mabuchi, A. Sekine, S. Saito, A. Takahashi, T. Tsunoda, Y. Nakamura, and K. Yamamoto. An intronic SNP in a RUNX1 binding site of SLC22A4, encoding an organic cation transporter, is associated with rheumatoid arthritis. *Nat Genet* **35**: 341–348 (2003).
65. V. D. Peltekova, R. F. Wintle, L. A. Rubin, C. I. Amos, Q. Huang, X. Gu, B. Newman, M. Van Oene, D. Cescon, G. Greenberg, A. M. Griffiths, P. H. St

George-Hyslop, and K. A. Siminovitch. Functional variants of OCTN cation transporter genes are associated with Crohn disease. *Nat Genet* **36**: 471–475 (2004).
66. M. Otsuka, T. Matsumoto, R. Morimoto, S. Arioka, H. Omote, and Y. Moriyama. A human transporter protein that mediates the final excretion step for toxic organic cations. *Proc Natl Acad Sci U S A* **102**: 17923–17928 (2005).
67. M. Hiasa, T. Matsumoto, T. Komatsu, and Y. Moriyama. Wide variety of locations for rodent MATE1, a transporter protein that mediates the final excretion step for toxic organic cations. *Am J Physiol Cell Physiol* **291**: C678–G686 (2006).
68. T. Terada, S. Masuda, J. Asaka, M. Tsuda, T. Katsura, and K. Inui. Molecular cloning, functional characterization and tissue distribution of rat H^+/organic cation antiporter MATE1. *Pharm Res* **23**: 1696–1701 (2006).
69. S. Masuda, T. Terada, A. Yonezawa, Y. Tanihara, K. Kishimoto, T. Katsura, O. Ogawa, and K. Inui. Identification and functional characterization of a new human kidney-specific H^+/organic cation antiporter, kidney-specific multidrug and toxin extrusion 2. *J Am Soc Nephrol* **17**: 2127–2135 (2006).
70. M. Tsuda, T. Terada, J. Asaka, M. Ueba, T. Katsura, and K. Inui. Oppositely-directed H^+ gradient functions as a driving force of rat H^+/organic cation antiporter MATE1. *Am J Physiol Renal Physiol* **292**: F593–F598 (2007).
71. M. Takano, K. Inui, T. Okano, H. Satio, and R. Hori. Carrier-mediated transport systems of tetraethylammonium in rat renal brush-border and basolateral membrane vesicles. *Biochim Biophys Acta* **773**: 113–124 (1984).
72. I. B. Roninson, J. E. Chin, K. G. Choi, P. Gros, D. E. Housman, A. Fojo, D. W. Shen, M. M. Gottesman, and I. Pastan. Isolation of human mdr DNA sequences amplified in multidrug-resistant KB carcinoma cells. *Proc Natl Acad Sci U S A* **83**: 4538–4542 (1986).
73. A. T. Fojo, K. Ueda, D. J. Slamon, D. G. Poplack, M. M. Gottesman, and I. Pastan. Expression of a multidrug-resistance gene in human tumors and tissues. *Proc Natl Acad Sci U S A* **84**: 265–269 (1987).
74. M. Dean, A. Rzhetsky, and R. Allikmets. The human ATP-binding cassette (ABC) transporter superfamily. *Genome Res* **11**: 1156–1166 (2001).
75. R. G. Deeley, C. Westlake, and S. P. Cole. Transmembrane transport of endo- and xenobiotics by mammalian ATP-binding cassette multidrug resistance proteins. *Physiol Rev* **86**: 849–899 (2006).
76. P. Krishnamurthy, and J. D. Schuetz. Role of ABCG2/BCRP in biology and medicine. *Annu Rev Pharmacol Toxicol* **46**: 381–410 (2006).
77. G. A. Altenberg. Structure of multidrug-resistance proteins of the ATP-binding cassette (ABC) superfamily. *Curr Med Chem Anticancer Agents* **4**: 53–62 (2004).
78. A. H. Schinkel, U. Mayer, E. Wagenaar, C. A. Mol, L. van Deemter, J. J. Smit, M. A. van der Valk, A. C. Voordouw, H. Spits, O. van Tellingen, J. M. Zijlmans, W. E. Fibbe, and P. Borst. Normal viability and altered pharmacokinetics in mice lacking mdr1-type (drug-transporting) P-glycoproteins. *Proc Natl Acad Sci U S A* **94**: 4028–4033 (1997).
79. M. F. Fromm. Importance of P-glycoprotein at blood-tissue barriers. *Trends Pharmacol Sci* **25**: 423–429 (2004).
80. C. G. Dietrich, A. Geier, and R. P. Oude Elferink. ABC of oral bioavailability: transporters as gatekeepers in the gut. *Gut* **52**: 1788–1795 (2003).
81. B. Greiner, M. Eichelbaum, P. Fritz, H. P. Kreichgauer, O. von Richter, J. Zundler, and H. K. Kroemer. The role of intestinal P-glycoprotein in the interaction of digoxin and rifampin. *J Clin Invest* **104**: 147–153 (1999).
82. K. Westphal, A. Weinbrenner, M. Zschiesche, G. Franke, M. Knoke, R. Oertel, P. Fritz, O. von Richter, R. Warzok, T. Hachenberg, H. M. Kauffmann, D. Schrenk, B. Terhaag, H. K. Kroemer, and W. Siegmund. Induction of P-glycoprotein by rifampin increases intestinal secretion of talinolol in human beings: a new type of drug/drug interaction. *Clin Pharmacol Ther* **68**: 345–355 (2000).

83. D. Durr, B. Stieger, G. A. Kullak-Ublick, K. M. Rentsch, H. C. Steinert, P. J. Meier, and K. Fattinger. St John's Wort induces intestinal P-glycoprotein/MDR1 and intestinal and hepatic CYP3A4. *Clin Pharmacol Ther* **68**: 598–604 (2000).
84. S. Masuda, and K. Inui. An up-date review on individualized dosage adjustment of calcineurin inhibitors in organ transplant patients. *Pharmacol Ther* **112**: 184–198 (2006).
85. T. Hashida, S. Masuda, S. Uemoto, H. Saito, K. Tanaka, and K. Inui. Pharmacokinetic and prognostic significance of intestinal MDR1 expression in recipients of living-donor liver transplantation. *Clin Pharmacol Ther* **69**: 308–316 (2001).
86. S. Masuda, M. Goto, M. Okuda, Y. Ogura, F. Oike, T. Kiuchi, K. Tanaka, and K. Inui. Initial dosage adjustment for oral administration of tacrolimus using the intestinal MDR1 level in living-donor liver transplant recipients. *Transplant Proc* **37**: 1728–1729 (2005).
87. S. Masuda, M. Goto, S. Fukatsu, M. Uesugi, Y. Ogura, F. Oike, T. Kiuchi, Y. Takada, K. Tanaka, and K. Inui. Intestinal MDR1/ABCB1 level at surgery as a risk factor of acute cellular rejection in living-donor liver transplant patients. *Clin Pharmacol Ther* **79**: 90–102 (2006).
88. H. Suzuki, and Y. Sugiyama. Excretion of GSSG and glutathione conjugates mediated by MRP1 and cMOAT/MRP2. *Semin Liver Dis* **18**: 359–376 (1998).
89. R. O. Elferink, and A. K. Groen. Genetic defects in hepatobiliary transport. *Biochim Biophys Acta* **1586**: 129–145 (2002).
90. G. L. Scheffer, M. Kool, M. de Haas, J. M. de Vree, A. C. Pijnenborg, D. K. Bosman, R. P. Elferink, P. van der Valk, P. Borst, and R. J. Scheper. Tissue distribution and induction of human multidrug resistant protein 3. *Lab Invest* **82**: 193–201 (2002).
91. T. Hirohashi, H. Suzuki, and Y. Sugiyama. Characterization of the transport properties of cloned rat multidrug resistance-associated protein 3 (MRP3). *J Biol Chem* **274**: 15181–15185 (1999).
92. T. Hirohashi, H. Suzuki, H. Takikawa, and Y. Sugiyama. ATP-dependent transport of bile salts by rat multidrug resistance-associated protein 3 (Mrp3). *J Biol Chem* **275**: 2905–2910 (2000).
93. N. Zelcer, K. van de Wetering, R. de Waart, G. L. Scheffer, H. U. Marschall, P. R. Wielinga, A. Kuil, C. Kunne, A. Smith, M. van der Valk, J. Wijnholds, R. O. Elferink, and P. Borst. Mice lacking Mrp3 (Abcc3) have normal bile salt transport, but altered hepatic transport of endogenous glucuronides. *J Hepatol* **44**: 768–775 (2006).
94. L. A. Doyle, and D. D. Ross. Multidrug resistance mediated by the breast cancer resistance protein BCRP (ABCG2). *Oncogene* **22**: 7340–7358 (2003).
95. J. D. Allen, S. C. Van Dort, M. Buitelaar, O. van Tellingen, and A. H. Schinkel. Mouse breast cancer resistance protein (Bcrp1/Abcg2) mediates etoposide resistance and transport, but etoposide oral availability is limited primarily by P-glycoprotein. *Cancer Res* **63**: 1339–1344 (2003).
96. J. W. Jonker, M. Buitelaar, E. Wagenaar, M. A. Van Der Valk, G. L. Scheffer, R. J. Scheper, T. Plosch, F. Kuipers, R. P. Elferink, H. Rosing, J. H. Beijnen, and A. H. Schinkel. The breast cancer resistance protein protects against a major chlorophyll-derived dietary phototoxin and protoporphyria. *Proc Natl Acad Sci U S A* **99**: 15649–15654 (2002).
97. G. Merino, J. W. Jonker, E. Wagenaar, A. E. van Herwaarden, and A. H. Schinkel. The breast cancer resistance protein (BCRP/ABCG2) affects pharmacokinetics, hepatobiliary excretion, and milk secretion of the antibiotic nitrofurantoin. *Mol Pharmacol* **67**: 1758–1764 (2005).

6. H^+/有機カチオンアンチポータ（MATE/SLC47A）

京都大学医学部附属病院薬剤部　寺田智祐
同教授　乾　賢一

key words　H^+/organic cation antiporter, renal secretion, brush-border membranes

動　向

腎臓における排泄は，糸球体濾過と尿細管分泌より構成されるが，薬物や代謝産物などの有機イオンは主に近位尿細管での分泌によって尿中に排泄される．近位尿細管での分泌過程は経上皮細胞的に進行し，血管側側底膜を介する細胞内への取り込みと，管腔側刷子縁膜を介する細胞内から管腔への放出という二段階の膜輸送によって支配されている[1,2]．たとえば，有機カチオンは側底膜の膜電位依存性有機カチオントランスポータによって細胞内に運ばれ，さらに刷子縁膜のH^+/有機カチオンアンチポータを介して能動的に管腔内へ分泌されることが知られている[3]．これまで，主に側底膜に発現する膜電位依存性の有機カチオントランスポータ（OCT1-3/SLC22A1-3）の構造，機能，発現に関する*in vitro*研究と，それらの分子情報を基盤とした臨床研究が進展してきた[4-8]．しかし，H^+/有機カチオンアンチポータの分子実体については未解明のまま残されており，その同定が待ち望まれていた．2005年に岡山大学の森山らのグループによって，大腸菌の多剤耐性に関与するmultidrug and toxin extrusion（MATE）の哺乳類ホモログとして，ヒト（h）およびマウス（m）のMATE1ならびにMATE2が同定された[9]．その後我々は，ラット(r)MATE1，hMATE1，hMATE2-KのcDNAを単離し[10,11]，その分子特性や薬物動態学的役割を明らかにしてきた．本稿では，MATEファミリーの遺伝子同定に至るまでの経緯と，両トランスポータの特徴について紹介する．

A. MATEがクローニングされるまで

1980年代前半より，腎膜小胞系や培養腎上皮細胞系などを用いて，側底膜ならびに刷子縁膜における有機カチオンの輸送機構が，生理あるいは薬物動態学的観点から解析されてきた．我々は，H^+/有機カチオンアンチポータが，逆向きのH^+勾配を駆動力とすること[12]，シメチジン（H_2ブロッカー）などのカチオン性薬物を基質にすること[13]などを実証し，その機能的特徴を明らかにしてきた．その後，1994年に，Gründemannら[14]が側底膜の有機カチオントランスポータOCT1を，また我々もそのアイソフォームであるOCT2を同定し[15]，腎臓における有機カチオン輸送の分子的解析はOCTを中心に進展してきた．しかし，その間も多くの研究者が，H^+/有機カチオンアンチポータの分子同定を試みてきたが，いずれも決定的な証拠を示すものではなかった．

最初の候補としては，ブタ由来の培養腎上皮細

胞LLC-PK_1から単離されたOCT2pがあげられる[16]．報告によると，基質特異性や阻害剤の感受性を基に，OCT2pがapical typeの有機カチオントランスポータであることが結論されている．しかし，その後の様々な種のOCT2の基質特異性や膜局在性などの解析によって，OCT2pはapical typeの有機カチオントランスポータではないと考えられている．

次に，有機イオントランスポータファミリーに属するOCTN1（SLC22A4）が，H^+/有機カチオンアンチポータとして機能していることが示唆された[17]．これは，OCTN1が腎尿細管刷子縁膜に局在することや，典型的な有機カチオンであるtetraethylammonium（TEA）をpH依存的に輸送したデータに基づいている．しかし，1) OCTN1を介したTEA輸送はelectrogenicであること[18]（古典的なH^+/有機カチオンアンチポータはelectroneutral），2) OCTN1 mRNAのヒト腎臓における発現はきわめて低いこと[19]，3) OCTN1の特異的基質として抗酸化物質であるergothioneineが見出され，その輸送活性はTEAよりもはるかに大きいこと[20]などから，少なくともOCTN1は従来，生理・薬物動態学的に示唆されてきたH^+/有機カチオンアンチポータの分子実体ではないと考えられている．

最後の候補としては，OCTN2（SLC22A5）があげられる．腎尿細管刷子縁膜に局在するOCTN2は，Na^+勾配を駆動力としてカルニチンの再吸収を媒介し，遺伝性全身カルニチン欠乏症の原因遺伝子として同定されている[21,22]．一方で，OCTN2は，Na^+非依存的にTEAを輸送すること[23]や，OCTN2を欠損している*jvs*マウスにおいてTEAの腎分泌クリアランスが低下すること[24]などから，OCTN2は刷子縁膜における有機カチオン輸送系としても機能していることが示唆されていた．しかし，我々は腎刷子縁膜小胞を用いた輸送実験によって，カルニチン輸送はTEA輸送とは独立していることを明らかにし，OCTN2の有機カチオン輸送への関与は小さいことを報告した[25]．したがって，OCTN2がH^+/有機カチオンアンチポータの分子実体であるという証拠は不充分であった．

このように，H^+/有機カチオンアンチポータとしていくつもの分子が候補としてあがってきたが，古典的なH^+/有機カチオンアンチポータの生化学的特性を完全に満たすものはなく，その分子実体は長年ベールに包まれていた．ところが，2005年に岡山大学の森山らのグループによって，大腸菌の多剤耐性に関与するMATEの哺乳類ホモログとして，ヒトおよびマウスのMATE1ならびにMATE2が同定された[9]．MATE1の臓器分布，膜局在ならびに輸送特性などから，本トランスポータが刷子縁膜においてH^+勾配によって駆動される輸送系として機能していることが示された．その後，我々の研究室を含め複数の研究室から，MATEの単離と機能解析が報告され，本トランスポータがH^+/有機カチオンアンチポータとして機能していることが実証されるに至った[10,11,26,27]．また，HUGO Gene Nomenclature Committeeによって，MATEはSLC47Aとして登録され，名実ともに重要なトランスポータとして位置付けられることになった．図1には，ヒト近位尿細管における有機カチオン輸送の模式図を示した．

B. MATE1の構造，臓器分布，膜局在

哺乳類のMATE1は現在，ヒト，マウス，ラットならびにウサギから同定されている[9-11,26,27]．ヒト，ラット，ウサギMATE1は，約570のアミノ酸からなるが，mMATE1は，C末端のアミノ酸配列が他種のMATE1よりも短く，532個のアミノ酸から構成されている[9,28]．ラットやウサギMATE1では13回膜貫通型タンパクであること

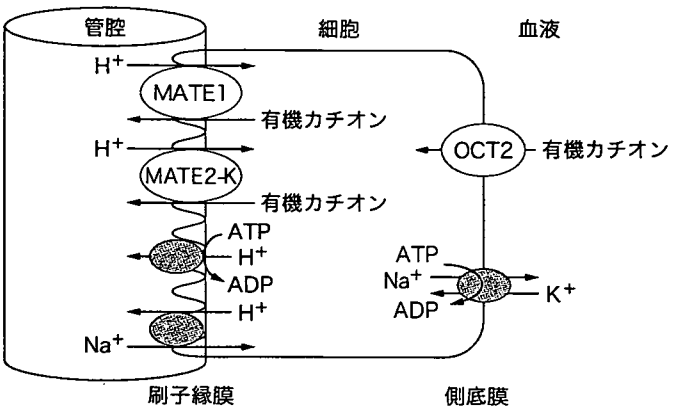

図1 ヒト近位尿細管における有機カチオン輸送

側底膜では，膜電位依存性のhOCT2が血管側から有機カチオンの取り込みを媒介し，刷子縁膜側では逆向きのH^+勾配を駆動力とするhMATE1やhMATE2-Kが細胞内の有機カチオンを管腔側へ排出する．H^+勾配はNa^+/H^+exchangerやH^+ポンプによって形成されている．

が推察されている[26,27]．いずれの種のMATE1も腎臓に発現し，microdissection法によるネフロン内分布の解析の結果，rMATE1 mRNAは近位曲尿細管および直尿細管に限局していることが判明した[11]．またreal-time PCR法によって，組織間の発現量の比較を行ったところ，hMATE1 mRNAは，腎臓，副腎＞＞精巣＞骨格筋，肝臓，子宮[10]に，またrMATE1 mRNAは，腎臓，胎盤＞膵臓＞脾臓[11]の順に発現していることがわかった．rMATE1は，ヒトやマウスで発現の認められた肝臓では発現していない．また特異抗体を用いた解析によって，MATE1は近位尿細管上皮細胞の刷子縁膜に局在していることが示されている[9,10,28,29]．

C. MATE2-Kの構造，臓器分布，膜局在

Otsukaらは，hMATE1 cDNAクローニング時に，hMATE2ならびにmMATE2 cDNAの報告を併せて行った[9]．我々は，hMATE2 cDNAの塩基配列を基にその遺伝子の増幅を試みたが，hMATE2 cDNAは単離されず，代わりにhMATE2-K cDNAを同定した[10]．*hMATE2-K*遺伝子は*hMATE2*遺伝子のエクソン7が108塩基短く，566個のアミノ酸をコードしている．hMATE1とのアミノ酸相同性は52%である．その後，Wrightらのグループも，ウサギ（rb）腎よりrbMATE2ではなく，rbMATE2-Kを同定し[27]，Otsukaらの報告したMATE2の機能や発現については現在のところ明らかにされていない．hMATE2-Kは腎特異的に発現し，近位尿細管上皮細胞の刷子縁膜に局在している．両トランスポータの特徴を表1にまとめた．

一方，mMATE2は，腎臓には発現しておらず，主に精巣に発現している[28]．また，森山らのグループは，mMATE2がMATE3のファミリーに分類されることをアミノ酸配列の相同性から提唱している[30]．アイソフォームとファミリーの名称が異なることは混乱をもたらす原因と考えられ，今後名称の統一が必要と考えられる．

表1 hMATE1, hMATE2およびhMATE2-Kの比較

	アミノ酸数	輸送活性	発現臓器*	膜局在	他の種でのアイソフォーム
hMATE1[9]	570	有	腎臓，肝臓など	刷子縁膜	マウス[9]，ラット[11,26]，ウサギ[27]
hMATE2[9]	602	?	腎臓のみ	?	?
hMATE2-K[10]	566	有	腎臓のみ	刷子縁膜	ウサギ[27]

*Otsukaらの論文では，Northern blottingによりhMATE2の腎臓での発現が示されているが，hMATE2-Kを検出している可能性も考えられる．またPCR産物長によりhMATE2とhMATE2-Kを区別するPCRを行ったところ，腎臓ではMATE2-Kのみ発現していた[10]．

D. MATEの薬物輸送特性

hMATE1ならびにhMATE2-Kは，尿細管分泌を受けるカチオン性薬物：メトホルミン（糖尿病治療薬），シメチジン（H_2ブロッカー），プロカインアミド（抗不整脈薬）などを顕著に輸送し，類似の薬物認識特性を示す[31]．これらhMATEsの基質認識特性および腎臓における発現分布は側底膜側hOCT2と類似しており，hOCT2を介して取り込まれた薬物はhMATE1やhMATE2-Kを介して尿細管管腔へ分泌されると考えられる．実際我々は，有機カチオン輸送系を有していないMDCK細胞をホストとしてhMATE1/hOCT2の共発現系を作製し，上述した薬物が尿細管分泌に対応した方向選択的な輸送を受けることを確認している．一方で，hMATE1は両性イオン型薬物であるセファレキシンを，またhMATE2-Kは白金系抗がん剤のオキサリプラチンをそれぞれ特異的に輸送し，両者の基質特異性に関する差異も見受けられた[31-33]．白金系抗がん剤の基質認識の異同については，腎毒性発現機構の観点から後述する．

E. MATEの駆動力と必須アミノ酸残基

これまで，腎刷子縁膜小胞を用いた輸送実験によって，H^+/有機カチオンアンチポータの駆動力は，逆向きのH^+勾配であることが示されていた[12,13]．実際，MATEを介したTEA取り込みは，細胞外pHがアルカリ側において高く，NH_4Cl処理による細胞内酸性化によって顕著に促進された[9-11]．しかし，いずれも間接的な証明であり，正確な輸送機序の解明には膜小胞を用いた解析が必須と考えられた．そこで，MATE1安定発現細胞からnitrogen cavitation法によって膜小胞を調製し，駆動力の直接的な証明を試みた[34]．その結果，TEAの取り込みは，逆向きのH^+勾配が存在するときのみ濃度勾配に逆らった上り坂輸送，すなわちオーバーシュート現象が観察された．さらにそのオーバーシュートは，プロトノフォアであるFCCP共存によって消失したことから，MATE1は逆向きのH^+勾配を駆動力とすることが判明した．またMATE1を介したTEA取り込みは膜電位の影響を受けなかったことから，H^+とTEAの化学量論比は1：1であることが推察された．

また，刷子縁膜小胞を用いた輸送解析より，H^+/有機カチオンアンチポータに存在するシステイン（Cys）やヒスチジン（His）残基が輸送機能に必須であることが示されていた[35,36]．またrMATE1の輸送活性は，Cys残基修飾試薬によって顕著に低下することが報告された[26]．そこで，rMATE1に存在するこれら必須アミノ酸残基の同定を試みたところ，MATE1の保存性Cysのうち，第1ならびに第3番目の膜貫通領域に存在す

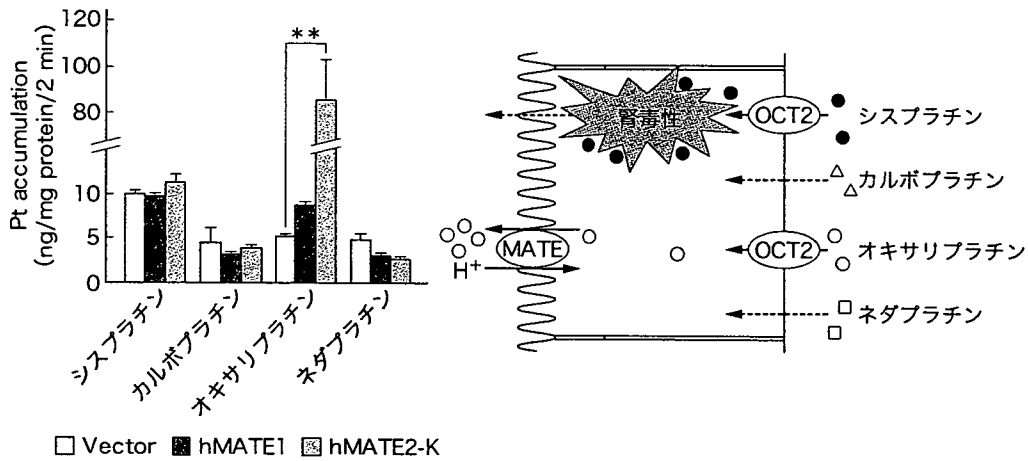

図2 MATEによる白金系抗がん剤の輸送特性と腎毒性発現機構

オキサリプラチンはOCT2によって腎尿細管に取り込まれるものの，MATEsによって効率的に尿中へ分泌されるため，腎蓄積性・腎毒性を示さない．一方，シスプラチンでは，MATEsによる分泌を受けないため腎臓に蓄積し，腎毒性を惹起する．カルボプラチンとネダプラチンは，OCT2やMATEsによって輸送されない．

るCys変異体，ならびに第10番目の膜貫通領域のHis変異体で輸送活性が低下した[37]．また，CysやHisのアミノ酸修飾試薬処理に及ぼす基質の保護効果について調べたところ，Cys残基は基質の結合部位として機能していることが示唆された．また7番目の膜貫通領域に存在するグルタミン酸も，輸送機能に重要な役割を果たしていることが示されている[9]．

F. hMATE1ならびにhMATE2-Kと腎毒性との関係

最後にhMATE1およびhMATE2-Kの機能と，白金系抗がん剤の腎毒性との関連について紹介する．本邦では現在，4種類の白金系抗がん剤（シスプラチン，オキサリプラチン，カルボプラチン，ネダプラチン）が承認されており，シスプラチンのみ高い腎蓄積と強い腎毒性を有することが知られている．その機序の一つとして，トランスポータによる白金系抗がん剤の腎動態制御が関与しているのではないかと考え検討を加えた．その結果，シスプラチンと腎毒性をほとんど示さないオキサリプラチンが，側底膜に発現するhOCT2によって有意に輸送されたが，カルボプラチンやネダプラチンの輸送は認められなかった[32]．一方，刷子縁膜側の輸送では，オキサリプラチンは両トランスポータにより顕著に輸送されたが(輸送活性：hMATE2-K＞hMATE1)，シスプラチンはいずれのトランスポータによっても輸送されなかった[32,33]．したがって，オキサリプラチンはOCT2によって腎尿細管に取り込まれるものの，MATEsによって効率的に尿中へ分泌されるため，腎蓄積性・腎毒性を示さないことがわかった（図2）．一方，シスプラチンでは，MATEsによる分泌を受けないため腎臓に蓄積し，その結果腎毒性を惹起することが示唆された（図2）．

むすび

長年，その分子実体が不明であった，H^+/有機カチオンアンチポータ（MATE/SLC47A）のcDNAがクローニングされ，これまで生理的に示されていたカチオン性薬物の腎排泄機構の全貌

が，ようやく分子的に理解されるようになった．事実，hMATE1/hOCT2共発現系の構築により，これまで適切な評価系のなかったヒトにおけるカチオン性薬物の尿細管分泌，薬物間相互作用そして腎毒性発現機構を，*in vitro*で解析可能になることは，医薬品開発や臨床の現場に多大なる有益な情報をもたらすものと考えられる．今後，MATEの調節機構や遺伝子多型に関する研究が進展することによって，本トランスポータの生理・薬物動態学的意義の解明がより一層進むことが期待される．

文献

1) Pritchard JB, Miller DS. Mechanisms mediating renal secretion of organic anions and cations. Physiol Rev. 1993; 73: 765-96.
2) Inui K, Okuda M. Cellular and molecular mechanisms of renal tubular secretion of organic anions and cations. Clin Exp Nephrol. 1998; 2: 100-8.
3) Inui K, Takano M, Hori R. Organic cation transport in the renal brush-border and basolateral membranes. In: Hatano M. editors. Nephrology. Tokyo: Springer-Verlag; 1991. p. 1391-8.
4) Inui K, Masuda S, Saito H. Cellular and molecular aspects of drug transport in the kidney. Kidney Int. 2000; 58: 944-58.
5) Burckhardt G, Wolff NA. Structure of renal organic anion and cation transporters. Am J Physiol Renal Physiol. 2000; 278: F853-66.
6) Jonker JW, Schinkel AH. Pharmacological and physiological functions of the polyspecific organic cation transporters: OCT1, 2, and 3 (SLC22A1-3). J Pharmacol Exp Ther. 2004; 308: 2-9.
7) Wright SH. Role of organic cation transporters in the renal handling of therapeutic agents and xenobiotics. Toxicol Appl Pharmacol. 2005; 204: 309-19.
8) Koepsell H, Lips K, Volk C. Polyspecific organic cation transporters: structure, function, physiological roles, and biopharmaceutical implications. Pharm Res. 2007; 24: 1227-51.
9) Otsuka M, Matsumoto T, Morimoto R, et al. A human transporter protein that mediates the final excretion step for toxic organic cations. Proc Natl Acad Sci USA. 2005; 102: 17923-8.
10) Masuda S, Terada T, Yonezawa A, et al. Identification and functional characterization of a new human kidney-specific H^+/organic cation antiporter, kidney-specific multidrug and toxin extrusion 2. J Am Soc Nephrol. 2006; 17: 2127-35.
11) Terada T, Masuda S, Asaka J, et al. Molecular cloning, functional characterization and tissue distribution of rat H^+/organic cation antiporter MATE1. Pharm Res. 2006; 23: 1696-701.
12) Takano M, Inui K, Okano T, et al. Carrier-mediated transport systems of tetraethylammonium in rat renal brush-border and basolateral membrane vesicles. Biochim Biophys Acta. 1984; 773: 113-24.
13) Takano M, Inui K, Okano T, et al. Cimetidine transport in rat renal brush border and basolateral membrane vesicles. Life Sci. 1985; 37: 1579-85.
14) Gründemann D, Gorboulev V, Gambaryan S, et al. Drug excretion mediated by a new prototype of polyspecific transporter. Nature. 1994; 372: 549-52.
15) Okuda M, Saito H, Urakami Y, et al. cDNA cloning and functional expression of a novel rat kidney organic cation transporter, OCT2. Biochem Biophys Res Commun. 1996; 224: 500-7.
16) Gründemann D, Babin-Ebell J, Martel F, et al. Primary structure and functional expression of the apical organic cation transporter from kidney epithelial LLC-PK_1 cells. J Biol Chem. 1997; 272: 10408-13.
17) Tamai I, Yabuuchi H, Nezu J, et al. Cloning and characterization of a novel human pH-dependent organic cation transporter, OCTN1. FEBS Lett. 1997; 419: 107-11.
18) Tamai I, Nakanishi T, Kobayashi D, et al. Involvement of OCTN1 (SLC22A4) in pH-dependent transport of organic cations. Mol Pharm. 2004; 1: 57-66.
19) Motohashi H, Sakurai Y, Saito H, et al. Gene

expression levels and immunolocalization of organic ion transporters in the human kidney. J Am Soc Nephrol. 2002; 13: 866-74.
20) Gründemann D, Harlfinger S, Golz S, et al. Discovery of the ergothioneine transporter. Proc Natl Acad Sci USA. 2005; 102: 5256-61.
21) Tamai I, Ohashi R, Nezu J, et al. Molecular and functional identification of sodium ion-dependent, high affinity human carnitine transporter OCTN2. J Biol Chem. 1998; 273: 20378-82.
22) Nezu J, Tamai I, Oku A, et al. Primary systemic carnitine deficiency is caused by mutations in a gene encoding sodium ion-dependent carnitine transporter. Nature Genet. 1999; 21: 91-4.
23) Ohashi R, Tamai I, Yabuuchi H, et al. Na^+-dependent carnitine transport by organic cation transporter (OCTN2): its pharmacological and toxicological relevance. J Pharmacol Exp Ther. 1999; 291: 778-84.
24) Ohashi R, Tamai I, Nezu J, et al. Molecular and physiological evidence for multifunctionality of carnitine/organic cation transporter OCTN2. Mol Pharmacol. 2001; 59: 358-66.
25) Ohnishi S, Saito H, Fukada A, et al. Distinct transport activity of tetraethylammonium from L-carnitine in rat renal brush-border membranes. Biochim Biophys Acta. 2003; 1609: 218-24.
26) Ohta K, Inoue K, Hayashi Y, et al. Molecular identification and functional characterization of rat multidrug and toxin extrusion type transporter 1 as an organic cation/H^+ antiporter in the kidney. Drug Metab Dispos. 2006; 34: 1868-74.
27) Zhang X, Cherrington NJ, Wright SH. Molecular identification and functional characterization of rabbit MATE1 and MATE2-K. Am J Physiol Renal Physiol. 2007; 293: F360-70.
28) Hiasa M, Matsumoto T, Komatsu T, et al. Wide variety of locations for rodent MATE1, a transporter protein that mediates the final excretion step for toxic organic cations. Am J Physiol Cell Physiol. 2006; 291: C678-86.
29) Nishihara K, Masuda S, Ji L, et al. Pharmacokinetic significance of luminal multidrug and toxin extrusion 1 in chronic renal failure rats. Biochem Pharmacol. 2007; 73: 1482-90.
30) Omote H, Hiasa M, Matsumoto T, et al. The MATE proteins as fundamental transporters of metabolic and xenobiotic organic cations. Trends Pharmacol Sci. 2006; 27: 587-93.
31) Tanihara Y, Masuda S, Sato T, et al. Substrate specificity of MATE1 and MATE2-K, human multidrug and toxin extrusions/H^+-organic cation antiporters. Biochem Pharmacol. 2007; 74: 359-71.
32) Yonezawa A, Masuda S, Yokoo S, et al. Cisplatin and oxaliplatin, but not carboplatin and nedaplatin, are substrates for human organic cation transporters (SLC22A1-3 and multidrug and toxin extrusion family). J Pharmacol Exp Ther. 2006; 319: 879-86.
33) Yokoo S, Yonezawa A, Masuda S, et al. Differential contribution of organic cation transporters, OCT2 and MATE1, in platinum agent-induced nephrotoxicity. Biochem Pharmacol. 2007; 74: 477-87.
34) Tsuda M, Terada T, Asaka J, et al. Oppositely directed H^+ gradient functions as a driving force of rat H^+/organic cation antiporter MATE1. Am J Physiol Renal Physiol. 2007; 292: F593-8.
35) Hori R, Maegawa H, Kato M, et al. Inhibitory effect of diethyl pyrocarbonate on the H^+/organic cation antiport system in rat renal brush-border membranes. J Biol Chem. 1989; 264: 12232-7.
36) Hori R, Maegawa H, Okano T, et al. Effect of sulfhydryl reagents on tetraethylammonium transport in rat renal brush border membranes. J Pharmacol Exp Ther. 1987; 241: 1010-6.
37) Asaka J, Terada T, Tsuda M, et al. Identification of essential histidine and cysteine residues of the H^+/organic cation antiporter multidrug and toxin extrusion (MATE). Mol Pharmacol. 2007; 71: 1487-93.
38) Yonezawa A, Masuda S, Nishihara K, et al. Association between tubular toxicity of cisplatin and expression of organic cation transporter rOCT2 (Slc22a2) in the rat. Biochem Pharmacol. 2005; 70: 1823-31.

Am J Physiol Renal Physiol 61: F593–F598, 2007.
First published October 17, 2006; doi:10.1152/ajprenal.00312.2006.

Oppositely directed H^+ gradient functions as a driving force of rat H^+/organic cation antiporter MATE1

Masahiro Tsuda, Tomohiro Terada, Jun-ichi Asaka, Miki Ueba, Toshiya Katsura, and Ken-ichi Inui

Department of Pharmacy, Kyoto University Hospital, Faculty of Medicine, Kyoto University, Kyoto, Japan

Submitted 9 August 2006; accepted in final form 14 October 2006

Tsuda M, Terada T, Asaka J-i, Ueba M, Katsura T, Inui K-i. Oppositely directed H^+ gradient functions as a driving force of rat H^+/organic cation antiporter MATE1. *Am J Physiol Renal Physiol* 292: F593–F598, 2007. First published October 17, 2006; doi:10.1152/ajprenal.00312.2006.—Recently, we have isolated the rat (r) H^+/organic cation antiporter multidrug and toxin extrusion 1 (MATE1) and reported its tissue distribution and transport characteristics. Functional characterization suggested that an oppositely directed H^+ gradient serves as a driving force for the transport of a prototypical organic cation, tetraethylammonium, by MATE1, but there is no direct evidence to prove this. In the present study, therefore, we elucidated the driving force of tetraethylammonium transport via rMATE1 using plasma membrane vesicles isolated from HEK293 cells stably expressing rMATE1 (HEK-rMATE1 cells). A 70-kDa rMATE1 protein was confirmed to exist in HEK-rMATE1 cells, and the transport of various organic cations including [^{14}C]tetraethylammonium was stimulated in intracellular acidified HEK-rMATE1 cells but not mock cells. The transport of [^{14}C]tetraethylammonium in membrane vesicles from HEK-rMATE1 cells exhibited the overshoot phenomenon only when there was an outwardly directed H^+ gradient, as observed in rat renal brush-border membrane vesicles. The overshoot phenomenon was not observed in the vesicles from mock cells. The stimulated [^{14}C]tetraethylammonium uptake by an H^+ gradient [intravesicular H^+ concentration ($[H^+]_{in}$) > extravesicular H^+ concentration ($[H^+]_{out}$)] was significantly reduced in the presence of a protonophore, carbonyl cyanide *p*-trifluoromethoxyphenylhydrazone (FCCP). [^{14}C]tetraethylammonium uptake was not changed in the presence of valinomycin-induced membrane potential. These findings definitively indicate that an oppositely directed H^+ gradient serves as a driving force of tetraethylammonium transport via rMATE1, and this is the first demonstration to identify the driving force of the MATE family. The present experimental strategy is very useful in identifying the driving force of cloned transporters whose driving force has not been evaluated.

multidrug and toxin extrusion 1; transporter; tetraethylammonium; renal secretion; membrane vesicles

THE SECRETION OF DRUGS AND xenobiotics is an important physiological function of the renal proximal tubules. Cationic drugs are secreted from blood to urine by cooperative functions of two distinct classes of organic cation transporters: one driven by the transmembrane potential difference in the basolateral membranes and the other driven by the transmembrane H^+ gradient in the brush-border membranes (7, 16). So far, several membrane potential-dependent organic cation transporters (OCT1–3) have been identified, and their physiological and pharmacokinetic roles have been evaluated (2, 5, 10). However, the molecular nature of H^+/organic cation antiport systems has remained to be elucidated.

Recently, Moriyama and co-workers (3, 15) have identified human (h) and mouse MATE1 and MATE2, which are orthologs of the multidrug and toxin extrusion (MATE) family of bacteria. They demonstrated that MATE1 was predominantly expressed at the luminal membranes of the urinary tubules and bile canaliculi and transported tetraethylammonium, a prototypical organic cation, in a pH-dependent manner (3, 15). We also isolated cDNAs for rat (r) MATE1 (20) and the human kidney-specific isoform MATE2-K (13). rMATE1 was significantly expressed in the kidney and placenta, but not in the liver, and real-time PCR analyses of microdissected nephron segments showed that rMATE1 was expressed in the proximal convoluted and straight tubules (20). On the other hand, hMATE2-K was only expressed in the kidney and was located at the brush-border membranes of renal proximal tubular cells (13). By conducting functional analyses, we showed that rMATE1 and hMATE2-K can transport a wide variety of organic cations including tetraethylammonium, N^1-methylnicotinamide, and metformin (13, 20). These characteristics of MATE1 are similar to those of the H^+/organic cation antiport system revealed by renal brush-border membrane vesicle studies (4, 14, 18, 19, 23).

MATE1 exhibited pH-dependent transport of tetraethylammonium in cellular uptake and efflux studies, and intracellular acidification by NH_4Cl pretreatment stimulated tetraethylammonium transport (3, 13, 15, 20), suggesting that MATE1 utilized an oppositely directed H^+ gradient as a driving force. However, these analyses are not enough to prove the H^+/tetraethylammonium antiport mechanism of MATE1, because it is possible that the pH-dependent transport of tetraethylammonium by MATE1 is regulated not by an H^+ gradient but by pH itself. Accordingly, in addition to the data obtained using the cell culture model, we need more direct evidence that an H^+ gradient is the driving force for MATE1.

In the present study, we developed HEK293 cells stably expressing rMATE1 (HEK-rMATE1 cells) and elucidated the driving force of rMATE1 by uptake studies using plasma membrane vesicles from HEK-rMATE1 cells for the first time.

MATERIALS AND METHODS

Materials. [^{14}C]levofloxacin (1.07 GBq/mmol) was kindly provided by Daiichi Pharmaceutical (Tokyo, Japan). [^{14}C]tetraethylammonium bromide (2.035 GBq/mmol), [^{14}C]creatinine (2.035 GBq/mmol), [^{14}C]procainamide (2.035 GBq/mmol), [^{3}H]quinidine (740 GBq/mmol), [^{3}H]quinine (740 GBq/mmol), L-[*N*-methyl-^{3}H]carnitine (3.145 TBq/mmol), and [*N*-methyl-^{14}C]nicotine (2.035 GBq/mmol) were obtained from American Radiolabeled Chemicals (St. Louis,

Address for reprint requests and other correspondence: K. Inui, Dept. of Pharmacy, Kyoto Univ. Hospital, Sakyo-ku, Kyoto 606-8507, Japan (e-mail: inui@kuhp.kyoto-u.ac.jp).

The costs of publication of this article were defrayed in part by the payment of page charges. The article must therefore be hereby marked "*advertisement*" in accordance with 18 U.S.C. Section 1734 solely to indicate this fact.

MO). [^{14}C]metformin (962 MBq/mmol), [^{14}C]guanidine hydrochloride (1.961 GBq/mmol), [8-^{3}H]acyclovir (110 GBq/mmol), and [8-^{3}H]ganciclovir (370 GBq/mmol) were purchased from Moravec Biochemicals (Brea, CA). [^{3}H]1-methyl-4-phenylpyridinium acetate (2.7 TBq/mmol), [^{3}H]estrone sulfate ammonium salt (2.1 TBq/mmol), and [^{14}C]*p*-aminohippurate (1.9 GBq/mmol) were purchased PerkinElmer Life Analytical Sciences (Boton, MA). [*N*-methyl-^{3}H]cimetidine (451 GBq/mmol) was obtained from Amersham Biosciences (Uppsala, Sweden). All other chemicals used were of the highest purity available.

Cell culture and transfection. HEK293 cells (American Type Culture Collection CRL-1573) were cultured in complete medium consisting of Dulbecco's modified Eagle's medium with 10% fetal bovine serum in an atmosphere of 5% CO_2-95% air at 37°C. pcDNA 3.1 (+) containing cDNA encoding rMATE1 or empty vector was transfected into HEK293 cells using LipofectAMINE 2000 Reagent (Invitrogen) according to the manufacturer's instructions. At 48 h after transfection, the cells were split in complete medium containing G418 (0.5 mg/ml, Nacalai Tesque, Kyoto, Japan) at a dilution of 1:200. Fifteen days after transfection, single colonies were picked out. Cells expressing rMATE1 (HEK-rMATE1 cells) were selected by measuring [^{14}C]tetraethylammonium uptake. Cells transfected with empty vector (HEK-pcDNA cells) were used as controls. These transfectants were maintained in complete medium with G418 (0.5 mg/ml).

Uptake experiments by HEK-rMATE1 cells. The cellular uptake of [^{14}C]tetraethylammonium was measured by using monolayers grown on poly-D-lysine-coated 24-well plates as reported previously with some modifications (13, 20, 22). Briefly, the cells were preincubated with 0.2 ml of incubation medium, pH 7.4 (in mM: 145 NaCl, 3 KCl, 1 $CaCl_2$, 0.5 $MgCl_2$, 5 D-glucose, and 5 HEPES) containing 30 mM NH_4Cl for 20 min at 37°C. The medium was then removed, and 0.2 ml of incubation medium (pH 7.4) containing each radiolabeled compound was added. After an appropriate period of incubation, the medium was aspirated, and the monolayers were rapidly washed twice with 1 ml of ice-cold incubation medium (pH 7.4). The cells were solubilized in 0.5 ml of 0.5 N NaOH, and then the radioactivity in aliquots was determined by liquid scintillation counting. The protein content of the solubilized cells was determined by the method of Bradford (1) using a Bio-Rad Protein Assay Kit (Bio-Rad Laboratories, Hercules, CA) with bovine γ-globulin as a standard.

Preparation of membrane vesicles from HEK-rMATE1 cells. Plasma membrane vesicles were prepared according to previous reports (6, 9). HEK-rMATE1 or HEK-pcDNA cells were seeded on 100-mm plastic dishes (4×10^6 cells/dish), and 20 or 40 dishes were used to prepare membrane vesicles in a single preparation. All procedures were performed at 4°C. At the third day after seeding, HEK-rMATE1 or HEK-pcDNA cells were washed with PBS and scraped with a rubber policeman into PBS. The cell suspension was centrifuged at 200 *g* for 10 min, suspended in 20 ml of PBS, and recentrifuged at 200 *g* for 10 min. The packed cell pellet was resuspended in 20 vol of 250 mM mannitol/10 mM HEPES-Tris (pH 7.5)/0.5 mM $MgCl_2$ (*buffer A*), and the cells were gently suspended with five strokes of a loose-fitting Dounce homogenizer. The washed cell suspension was placed in a nitrogen cavitation bomb (Parr Instrument) at 700 lb/in.^{2} for 15 min. After the homogenate was collected, K_2EDTA (pH 7.5) was added to a final concentration of 1 mM. The homogenate was centrifuged at 750 *g* for 15 min, and the supernatant was centrifuged at 20,000 *g* for 15 min. The supernatant was centrifuged at 100,000 *g* for 60 min. The pellet was resuspended in 100 mM mannitol/10 mM MES-KOH (pH 6.0; experimental buffer) or 100 mM mannitol/10 mM HEPES-KOH (pH 7.5; experimental buffer) and centrifuged again at 100,000 *g* for 60 min. The pellet was suspended in the same experimental buffer (pH 6.0 or 7.5) by sucking the suspension 10 times through a fine needle (~4–10 mg protein/ml). KCl (pH 6.0 or 7.5) was added to a final concentration of 100 mM.

Transport experiments by membrane vesicles. The uptake of [^{14}C]tetraethylammonium by membrane vesicles was measured by a rapid filtration technique with a slight modification (8, 19). In the regular assays, the reaction was initiated rapidly by adding 80 μl of buffer, containing 31.25 μM [^{14}C]tetraethylammonium, to 20 μl of membrane vesicle suspension at 25°C. After specified periods, the incubation was terminated by diluting the reaction mixture with 1 ml of ice-cold stop solution containing (in mM) 150 KCl, 20 HEPES-Tris (pH 7.5), 0.1 $HgCl_2$, and 1 tetraethylammonium. The mixture was poured immediately onto Millipore filters (HAWP, 0.45 μm, 2.5 cm in diameter), and the filters were washed with 5 ml of ice-cold stop solution. The radioactivity of [^{14}C]tetraethylammonium trapped in membrane vesicles was determined using an ACS II (Amersham Biosciences) by liquid scintillation counting. The protein content was determined by the method of Bradford (1) using a Bio-Rad Protein Assay Kit (Bio-Rad Laboratories) with bovine γ-globulin as a standard.

Western blot analysis. Polyclonal antibody was raised against a synthetic peptide corresponding to the intracellular domain of rMATE1 (CQQAQVHANLKVN, no. 465–477) (13). Brush-border membrane vesicles from rat kidney cortex were prepared as described previously (12). Membrane fractions were separated by SDS-PAGE and analyzed by Western blotting as described previously (17, 21).

Data analysis. Data were analyzed statistically with a one-way analysis of variance followed by Scheffé's test and are expressed as means ± SE.

RESULTS

Generation of HEK-rMATE1 cells. First, we generated and characterized HEK293 cells stably expressing rMATE1. As shown in Fig. 1, an immunoreactive protein with a molecular weight of ~70 kDa was detected in HEK-rMATE1 cells and rat renal brush-border membranes but not in HEK-pcDNA cells. The functional expression of rMATE1 was assessed by measuring the

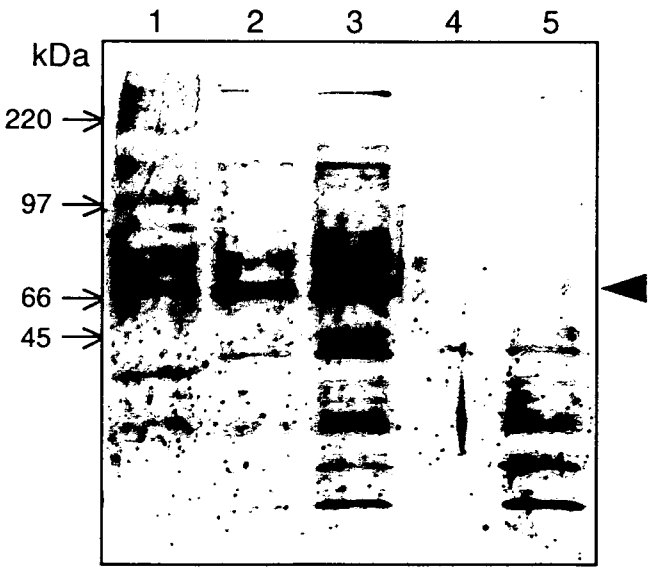

Fig. 1. Western blot analysis of rat renal brush-border membranes and plasma membranes obtained from HEK-rat multidrug and toxin extrusion 1(rMATE1) and HEK-pcDNA cells. Renal brush-border membranes (20 μg) and plasma membranes (5 or 20 μg) obtained from HEK-rMATE1 and HEK-pcDNA cells were separated by SDS-PAGE (10%) and blotted onto polyvinylidene difluoride membranes. The antiserum for rMATE1 (1:1,000) was used as a primary antibody. A horseradish peroxidase-conjugated anti-rabbit IgG antibody was used for detection of bound antibodies, and the strips of blots were visualized by chemiluminescence on X-ray film. The arrowhead indicates the position of rMATE1. Lanes were as follows: *lane 1*, rat renal brush-border membranes; *lane 2*, HEK-rMATE1 (5 μg); *lane 3*, HEK-rMATE1 (20 μg); *lane 4*, HEK-pcDNA (5 μg); and *lane 5*, HEK-pcDNA (20 μg).

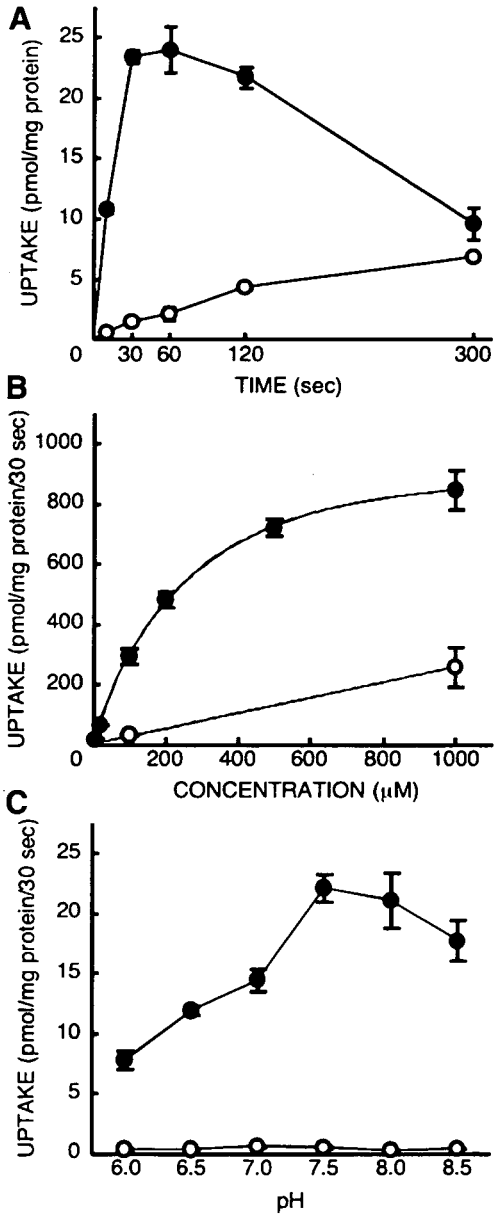

Fig. 2. Transport of [^{14}C]tetraethylammonium (TEA) by HEK-rMATE1 cells. *A*: time course of [^{14}C]TEA uptake by HEK-rMATE1 and HEK-pcDNA cells. HEK-rMATE1 cells (●) and HEK-pcDNA cells (○) were preincubated with 30 mM NH_4Cl (pH 7.4) for 20 min. Then, the preincubation medium was removed, and the cells were incubated with 5 μM of [^{14}C]TEA (pH 7.4) for indicated time at 37°C. Each point represents the mean ± SE of 3 monolayers. This figure is representative of 3 separate experiments. *B*: concentration dependence of [^{14}C]TEA uptake by HEK-rMATE1 cells. HEK-rMATE1 cells were preincubated with 30 mM NH_4Cl (pH 7.4) for 20 min. Then, the preincubation medium was removed, and the cells were incubated with various concentration of [^{14}C]TEA (pH 7.4) in the absence (●) or presence (○) of 5 mM TEA for 30 s at 37°C. Each point represents the mean ± SE of 3 monolayers. *C*: effect of extracellular pH on [^{14}C]TEA uptake by HEK-rMATE1 and HEK-pcDNA cells. HEK-rMATE1 cells (●) and HEK-pcDNA cells (○) were preincubated with 30 mM NH_4Cl (pH 7.4) for 20 min. Then, the preincubation medium was removed, and the cells were incubated with 5 μM of [^{14}C]TEA (indicated pH) for 30 s at 37°C. Each point represents the mean ± SE of 3 monolayers. The figure is representative of 2 separate experiments.

uptake of [^{14}C]tetraethylammonium in the HEK-rMATE1 cells under the intracellular acidified conditions caused by NH_4Cl pretreatment. A time- and concentration-dependent uptake of [^{14}C]tetraethylammonium by HEK-rMATE1 cells was observed (Fig. 2, *A* and *B*). [^{14}C]tetraethylammonium uptake by HEK-rMATE1 cells exhibited saturable kinetics, and an apparent K_m value of 304 ± 80 μM was calculated from three separate experiments. When the extracellular pH was changed from 6.0 to 8.5, a bell-shaped pH profile of [^{14}C]tetraethylammonium uptake via rMATE1 was observed, and the uptake was greatest at pH 7.5 and lowest at pH 6.0 (Fig. 2*C*).

Uptake of various compounds by HEK-rMATE1 cells. We then examined the substrate specificity of rMATE1. As shown in Fig. 3, rMATE1 mediated the transport of various organic cations with different chemical structures such as [^{14}C]tetraethylammonium, [^{3}H]1-methyl-4-phenylpyridinium acetate, [^{3}H]cimetidine, and [^{14}C]metformin. The transport of other organic cations such as [^{14}C]procainamide, [^{14}C]creatinine, and [^{14}C]guanidine was greater in HEK-rMATE1 cells than in HEK-pcDNA cells, although the stimulation was not remarkable.

Characteristics of [^{14}C]tetraethylammonium transport by membrane vesicles from HEK-rMATE1 cells. Next, we performed transport experiments using plasma membrane vesicles isolated from HEK-rMATE1 cells and HEK-pcDNA cells. In the presence of an H^+ gradient [intravesicular H^+ concentration ($[H^+]_{in}$) > extravesicular H^+ concentration ($[H^+]_{out}$)], a marked

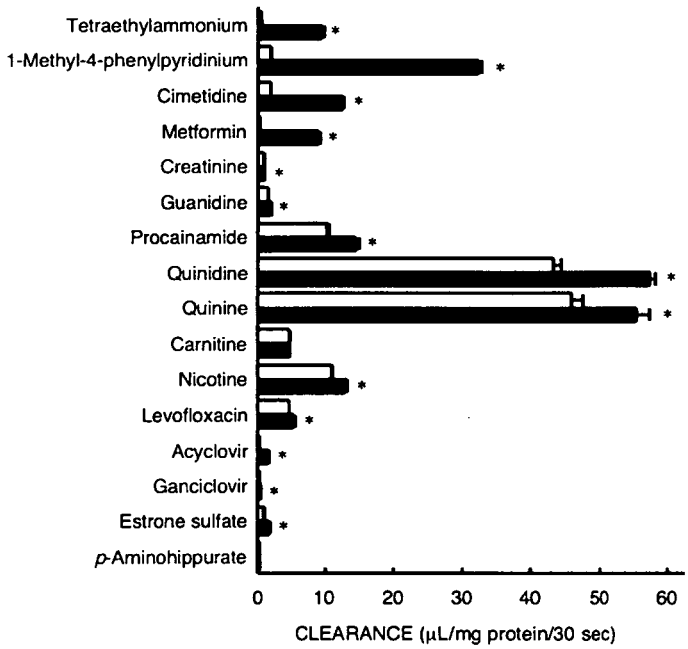

Fig. 3. Uptake of various compounds by HEK-rMATE1 cells. HEK-pcDNA cells (open bars) and HEK-rMATE1 cells (filled bars) were preincubated with 30 mM NH_4Cl (pH 7.4) for 20 min. Then, the preincubation medium was removed, and the cells were incubated with [^{14}C]TEA (5 μM), [^{3}H]1-methyl-4-phenylpyridinium acetate (3.8 nM), [^{3}H]cimetidine (11.1 nM), [^{14}C]metformin (10 μM), [^{14}C]creatinine (5 μM), [^{14}C]guanidine hydrochloride (5 μM), [^{14}C]procainamide (5 μM), [^{3}H]quinidine (13.9 nM), [^{3}H]quinine (13.9 nM), [^{3}H]carnitine (3.3 nM), [^{14}C]nicotine (5 μM), [^{14}C]levofloxacin (14 μM), [^{3}H]acyclovir (92 nM), [^{3}H]ganciclovir (28 nM), [^{3}H]estrone sulfate (4.86 nM), or [^{14}C]*p*-aminohippurate (5 μM) for 30 s at 37°C. Each bar represents the mean ± SE of 3 monolayers. The figure is representative of 2 separate experiments. *$P < 0.05$ significantly different from HEK-pcDNA cells.

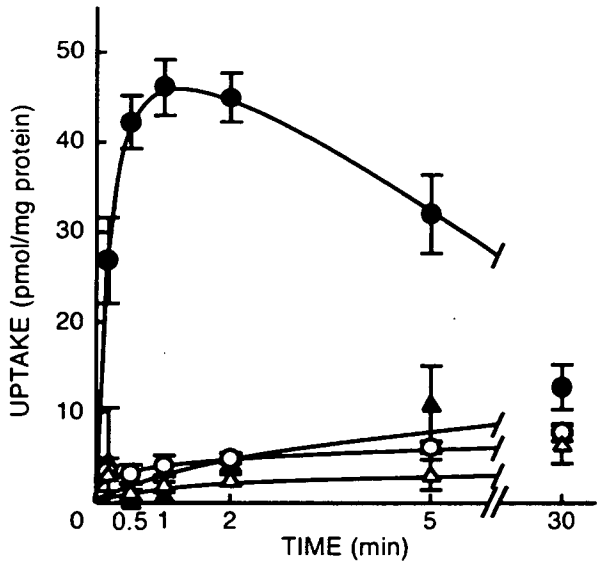

Fig. 4. Time course of [^{14}C]TEA uptake by membrane vesicles from HEK-pcDNA and HEK-rMATE1 cells. The uptake of [^{14}C]TEA by membrane vesicles from HEK-pcDNA cells (○, △) and HEK-rMATE1 cells (●, ▲) was examined in the absence (○, ●) or presence (△, ▲) of 10 mM TEA. Membrane vesicles were prepared in the experimental buffer at pH 6.0. The uptake of [^{14}C]TEA was examined in the experimental buffer containing 31.25 μM [^{14}C]TEA and 100 mM KCl at pH 7.5 in the absence or presence of 10 mM TEA. Each point represents the mean ± SE of 3 determinations.

stimulation of [^{14}C]tetraethylammonium uptake (overshoot phenomenon) was observed in membrane vesicles from HEK-rMATE1 cells, but not in those from HEK-pcDNA cells (Fig. 4). The overshoot phenomenon disappeared in the presence of an excess of cold tetraethylammonium.

Driving force for [^{14}C]tetraethylammonium transport by membrane vesicles from HEK-rMATE1 cells. To elucidate the driving force of tetraethylammonium transport by rMATE1, we performed [^{14}C]tetraethylammonium transport experiments using membrane vesicles from HEK-rMATE1 cells. As shown in Fig. 5, the presence of an H^+ gradient ($[H^+]_{in} > [H^+]_{out}$) induced a marked stimulation of [^{14}C]tetraethylammonium uptake against the concentration gradient. On the other hand, no stimulation of [^{14}C]tetraethylammonium uptake was observed in the absence of the gradient or in the presence of the reverse gradient ($[H^+]_{in} < [H^+]_{out}$). The final amount of [^{14}C]tetraethylammonium taken up in the presence of the H^+ gradient ($[H^+]_{in} > [H^+]_{out}$) was not so different from that attained in the absence of the gradient or in the presence of the reverse gradient ($[H^+]_{in} < [H^+]_{out}$).

To further evaluate the effect of an outwardly directed H^+ gradient on [^{14}C]tetraethylammonium uptake, the influence of a protonophore, FCCP, was examined. As shown in Fig. 6*A*, the initial rate of [^{14}C]tetraethylammonium uptake in the presence of an H^+ gradient ($[H^+]_{in} > [H^+]_{out}$) was markedly

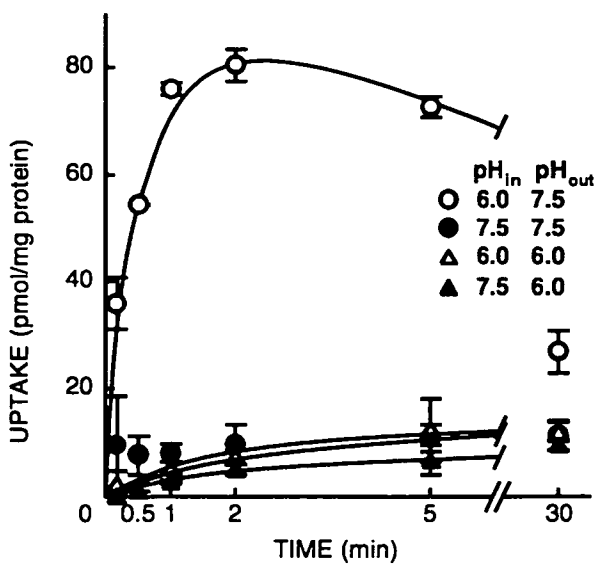

Fig. 5. Effect of H^+ gradient on [^{14}C]TEA uptake by membrane vesicles from HEK-rMATE1 cells. Membrane vesicles were prepared in the experimental buffer at pH 6.0 (○, △) or 7.5 (●, ▲). The uptake of [^{14}C]TEA was examined in the experimental buffer containing 31.25 μM [^{14}C]TEA and 100 mM KCl at pH 6.0 (△, ▲) or 7.5 (○, ●). Each point represents the mean ± SE of 3 determinations. The figure is representative of 2 separate experiments. pH_{in}, intravesicular pH; pH_{out}, extravesicular pH.

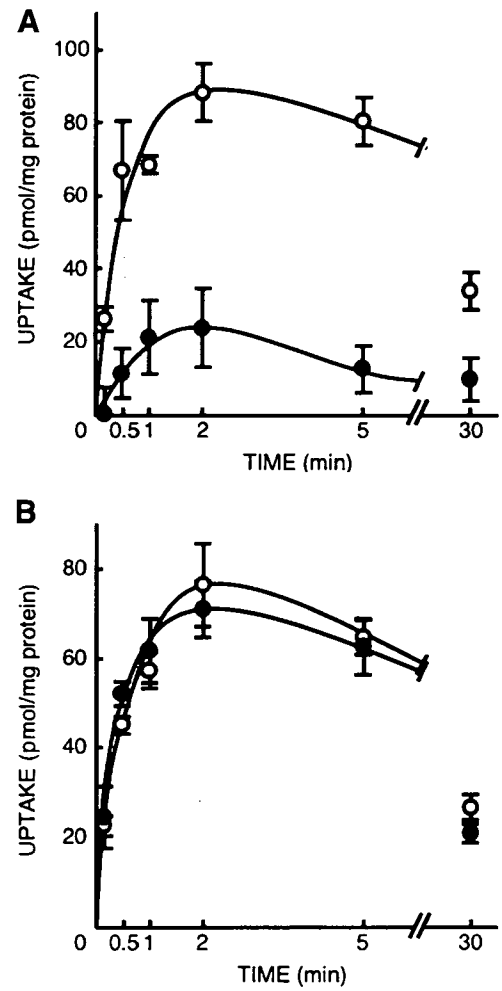

Fig. 6. Effect of FCCP (*A*) and valinomycin (*B*) on [^{14}C]TEA uptake in the presence of an outwardly directed H^+ gradient by membrane vesicles from HEK-rMATE1 cells. *A*: membrane vesicles were prepared in the experimental buffer at pH 6.0. The uptake of [^{14}C]TEA was examined in the experimental buffer containing 31.25 μM [^{14}C]TEA and 100 mM KCl at pH 7.5 in the absence (○) or presence (●) of 40 μM FCCP. Each point represents the mean ± SE of 3 determinations. The figure is a representative of 2 separate experiments. *B*: membrane vesicles were prepared in the experimental buffer at pH 6.0. The uptake of [^{14}C]TEA was examined in the experimental buffer containing 31.25 μM [^{14}C]TEA and 100 mM CsCl at pH 7.5 in the absence (○) or presence (●) of 8 μM valinomycin. Each point represents the mean ± SE of 3 determinations. The figure is representative of 2 separate experiments.